Li, X. and Chen, Q. 2021. "Development of a novel method to detect clothing level and facial skin temperature for controlling HVAC systems," *Energy and Buildings*, 239: 110859.

Development of a novel method to detect clothing level and facial skin temperature for controlling HVAC systems

Xuan Li[1], Qingyan Chen[1,*]
[1]School of Mechanical Engineering, Purdue University, 585 Purdue Mall, West Lafayette, IN, 47907, USA

*Corresponding author: Qingyan Chen, yanchen@purdue.edu

Abstract

People spend most of their time indoors, and thus it is important to provide occupants with a comfortable indoor thermal environment. However, inappropriate thermostat temperature settings in offices make occupants less comfortable. This study developed a new control strategy for HVAC systems that adjusts the thermostat setpoint according to clothing level and mean facial skin temperature. An image-classification model was trained on the basis of a convolutional neural network (CNN) to classify the clothing level of occupants, which was then used to calculate a comfortable air temperature. This investigation used a long-wave infrared (LWIR) camera with a face-detection program to obtain occupants' mean facial skin temperature. This study performed experimental tests to correlate mean facial skin temperature with thermal sensation votes. The mean facial skin temperature was then used to develop a control strategy for an HVAC system in a single-occupant office. With the use of the control strategy, 91% of the subjects tested in this investigation felt thermally neutral in the office.

Keywords

Thermal comfort, image classification, clothing level, infrared thermography, skin temperature, thermostat setpoint

1. Introduction

People spend 90% of their time indoors, and many spend their working hours in office environments [1]. Therefore, it is especially important to create healthy, comfortable, and productive indoor thermal environments. Nowadays, such environments are usually provided by heating, ventilation, and air conditioning (HVAC) systems. However, based on ASHRAE Global Thermal Comfort Database II, only 43% of the subjects reported neutral about their indoor environment [2].

Thermal comfort is a subjective evaluation of the thermal environment around a person [3]. Numerous models are available for the study of thermal comfort [4]. The most popular model is the predicted mean vote (PMV) and predicted percentage of dissatisfaction (PPD) developed by Fanger [5]. In their work, six factors: air temperature, relative humidity, air velocity, mean radiant temperature, metabolic rate and clothing level are considered have dominant impact over thermal comfort. However, as multiple studies [6-7] have observed, this model was developed for steady-

state conditions. Some researchers have used an adaptive concept to better explain thermal comfort in reality [8-9] and produced several effective models [10-13]. However, these models are limited to specific environments with variables such as air velocity and mean radiant temperature, which also diminishes their applicability. Therefore, many investigations started to use personalized parameters such as physiological parameters to characterize thermal comfort, such as local skin temperature [14-16], blood volume change [17], facial skin temperature [18-19], and heart rate [20-21]. These personal parameters are more precise indicators of thermal comfort and could therefore be used to control an HVAC system to make occupants more comfortable.

For automatic measurement of physiological parameters, the use of thermocouples or specialized equipment is not ideal. The recent development of wearable sensors for health monitoring has enabled non-invasive measurement of physiological parameters. [22-23]. However, these wearable sensors would also interfere with occupants' daily activities, and their accuracy is not consistent. Meanwhile, thermographic cameras are capable of measuring skin temperature. Because these cameras can be installed on walls and ceilings, they create less interference than the wearable sensors. Cosma and Simha [24-25] used a thermographic camera to measure local body temperature for the modeling of thermal comfort under transient conditions. Wang et al. [26] used an online learned thermal comfort model with infrared thermal imaging to control the thermal environment. Li et al. [23] employed infrared thermography to measure temperature at different locations on the face to predict thermal comfort. This information could be used to control an HVAC system and make occupants more thermally comfortable.

Meanwhile, many buildings use building automation systems (BAS) to control HVAC systems for room air temperature, which is usually determined by a thermostat [27]. However, the room air temperature setpoints which rarely got changed throughout a year were determined from a standard designed for specific clothing levels [28]. Therefore, when occupants' clothing level varied in a year [29], they would often feel uncomfortable in these indoor environments. Furthermore, studies have found that the current control method does not consider occupants' thermal comfort, and occupants usually make faulty adjustments to the temperature setpoint [30-31]. Such situations not only make occupants more uncomfortable but also result in the waste of energy by HVAC systems [32]. To solve these problems, it is necessary to devise a control system that provides a comfortable air temperature for different clothing levels and adjusts the temperature setpoint automatically according to occupants' thermal comfort.

To determine clothing level, most of the published studies have used questionnaires [33-34]. However, this method cannot obtain occupants' clothing level in a convenient or timely manner. Other studies have used numerical models to predict clothing level from the outdoor air temperature [35-37], but such models do not consider personal differences and cannot make real-time predictions. As machine learning has advanced, image classification has become available for clothing level identification. One study used a convolutional neural network (CNN) to determine clothing type (T-shirt, shoes, shorts, etc.) [38]. It may also be possible to use a CNN to determine clothing level.

This paper reports our use of a convolutional neural network to determine the clothing level of occupants, and our use of mean facial skin temperature to evaluate thermal comfort for the control of an HVAC system.

2. Method

This section describes the determination of clothing level from an image based on a CNN model. Then this section presents the identification of comfortable air temperatures for different clothing levels and our investigation of the relationship between mean facial skin temperature and thermal comfort. Finally, we present the development of a control strategy based on thermal sensation vote (TSV).

2.1 Clothing-level classification

This study used a CNN to determine clothing type. The CNN has several variations, and we adopted the MobileNetV2 [39] architecture to build a new CNN model for clothing-level classification with the use of transfer learning. Transfer learning employs a new dataset to modify a pre-trained neural network in order to solve new tasks. This type of learning not only saves time but also requires less computational power than building a new CNN model from scratch. Furthermore, this method preserves the performance of the original network because the original model is not modified.

We connected a pre-trained MobilNetV2 to a linear classifier in order to build the clothing-level classifier, the structure of which is shown in Fig. 1. When we used this structure, we did not have to train the whole MobileNetV2, which has millions of parameters; rather, we needed to train only the linear classifier, with thousands of parameters.

Figure 1. Structure of clothing-level classifier

To train the model, this study prepared 300 images for each clothing level, ranging from 0.3 *clo* to 0.8 *clo* with an increment of 0.1 *clo*, for a total of 1800 images. To build a clean and representative dataset, we applied the following rules: (1) the clothes should be fully visible, including the shoes, which contribute to the total clothing level; (2) the clothes should be of various colors, to avoid overfitting of the classifier model with clothing color; (3) the height, weight, gender, etc., of the subject in the image should not be restricted, again to prevent overfitting; (4) the composition of the image should be simple; and (5) the subject in the image should stand out against the background. This study followed the method in the ASHRAE handbook [3] to calculate the total clothing level for each image. Each image was categorized into a folder that was labeled with the corresponding clothing level.

The training dataset was then used to train the above-mentioned image classification model. This study used Python as the programming language and TensorFlow [40] as the machine learning library to train the new model. The training program used cross-entropy as the loss function. Cross-entropy is a technique to quantify the difference between two probability distributions [45]. In machine learning, this method was commonly used to determine the difference between the model predict distribution and the true distribution. Therefore, when using cross-entropy as the loss

function, the goal of training is to minimize the loss function to reduce the difference between predicted distribution and real distribution.

Since the goal of training was to minimize the loss function, we used mini-batch gradient descent. Table 1 lists the hyperparameter settings for the mini-batch gradient descent algorithm. The learning rate controlled the amount of updating the weight parameters in the model. The momentum was a constant value that would accelerate the training and prevent a local minimum; the most common value for the momentum was 0.9 [41]. The batch size was the number of samples used to update the model one time. A batch size of 32 was the most common setting [41]. Lastly, the epoch indicates the number of times the program trained over the full training group.

Table 1. Hyperparameters for mini-batch gradient descent.

Hyperparameter	Value
Learning rate	0.0025
Momentum	0.9
Batch size	32
Epochs	60

By running the training program with these hyperparameters, the program identified a model that could be used to perform clothing-level classification. The model was tested with the use of images captured in offices. If the classification model was able to predict most of the input images, then it would be reasonable to conclude that the CNN could feasibly be used to measure clothing level. Note that the aim of this study was to find if the proposed method would be able to correlate the clothing level with the images. The accuracy needs further validation in the future.

2.2 Comfortable air temperature

To determine comfortable air temperatures for different clothing levels, this study collected data on air temperature, clothing level, and thermal sensation in a single-occupant office at Purdue University. Fig. 2 shows the office layout used for the tests. This office had one exterior wall with a double-pane window and the other surfaces were interior. The exterior wall and windows were well insulated because this building was designed as a high-performance building built in 2013 with LEED-Gold certified. Such high-performance building also provided a good RH within the comfortable range mentioned in [3] in each office. A drapery was lowered during the tests. Thus, the radiation was not a major concern.

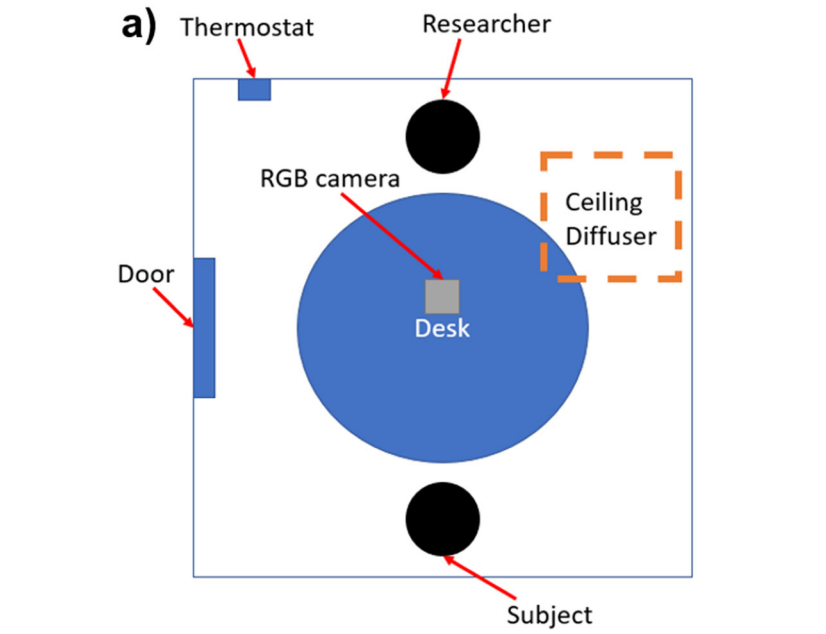

Figure 2. Room layout (a) preparation room (b) test room

This office contained a thermostat (Siemens 544–760A) as shown in Fig. 3(a) that was connected to a building automation system (BAS) to control the room air temperature. The thermostat had an adjustment range from 18.3°C to 26.7°C. A data logger (Sper Scientific 800,049) as shown in Fig. 3(b) was used to record minute-by-minute air temperature in the office during the tests. The system had an accuracy of ±0.6°C and had featured automatic baseline calibration to calibrate the equipment each time the unit was turned on. An RGB camera (Logitech C920) as shown in Fig. 3(c), with a resolution of full HD (1080p), was placed in preparation room shown as Fig. 2(a) and it was used to capture images of the occupant for clothing-level classification. For validation of the classification results, the occupant reported his or her actual clothing level. If the self-reported clothing level was different from that of the classification program, the self-reported value was

used as the true value. For understanding of the subject's comfort level, his or her thermal sensation was recorded on a questionnaire using the seven-point TSV scale (-3 for cold, -2 for cool, -1 for slightly cool, 0 for neutral, +1 for slightly warm, +2 for warm, and +3 for hot) [3].

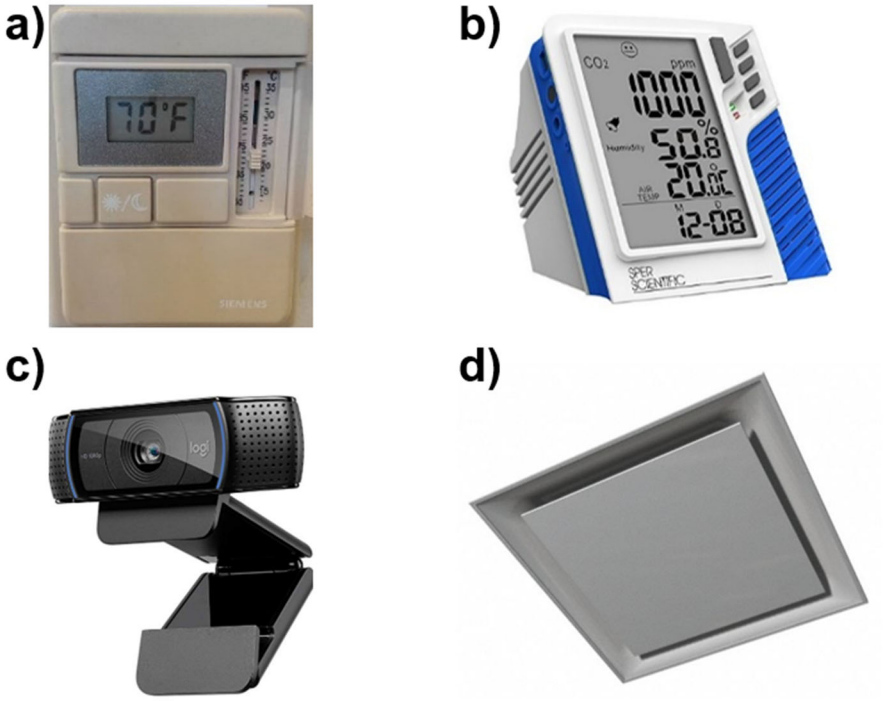

Figure 3. Experiment equipment (a) thermostat, (b) data logger, (c) RGB camera, and (d) air diffuser.

To determine the comfortable air temperature, this study assumed that (1) the air velocity around the occupant in the office was below 0.2 m/s, so that the draft effect on the occupant was minimal [3]. Fig. 3(d) shows the air diffuser used in both the preparation and the test room. Because the diffuser in the experiment room discharged air horizontally and the airflow was attached to the ceiling due to Coanda effect and the air did not go downwards since the inlet was not a hole, this assumption was reasonable for our experiment setup. However, it needs to be considered in other circumstances where the air is blowing to the occupant; (2) the mean radiant temperature around the occupant was the same as the air temperature, and the RH in the office was within the comfortable range of 30% to 70% [3]; and (3) all the occupants involved in the data collection were in a sedentary state and performed office work during the investigation, so that their metabolism rates were similar. Table 2 provides information on whether the factors related to thermal comfort based on Fanger's model [11] is measured or assumed in this study

Table 2. Measurement of factors impacting thermal comfort

Factor	**Measured/Assumed**
Air temperature	Measured via Data logger
Relative humidity	Measured via Data logger

Air velocity	Assumed to be <0.2 m/s
Mean radiant temperature	Assumed to have minimal impact (verified via LWIR camera)
Clothing level	Measured via CNN model
Metabolic rate	Assumed to be at sedentary

The procedure for collection of comfortable air temperature data at different clothing levels was as follows. The experiment started at the preparation room with layout shown as Fig. 2(a). In the preparation room, each subject was provided with instructions for reporting TSV based on the seven-point scale and assured they did not involve in physical exercises to maintain similar metabolic rate among different subjects. Next, an image of the subject was captured with the RGB camera to determine the clothing level. The subject then entered the office, shown as Fig. 2(b) without changing the clothing level, in which the air temperature was controlled at 20°C. After a 10-minute acclimation period [42] in the office, the subject reported the first TSV. The subject could then increase the thermostat setpoint by 1 K if the subject felt cold and decrease the setpoint by 1 K if the subject felt warm. After the air temperature reached the new setpoint, the subject reported another TSV. If the subjects were still not comfortable, her or she could adjust the thermostat to new air temperature and provide another TSV, until TSV = 0 (neutral) was finally reached. The air temperature at that time was regarded as the comfortable air temperature setpoint for the subject's clothing level. In this experiment, we intended to correlate occupant's clothing level and air temperature, thus, we did not measure the mean facial skin temperature using the LWIR camera. From this dataset, we could determine HVAC setpoints that suit different clothing levels.

2.3 Relationship between mean facial skin temperature and thermal comfort

To correlate the comfortable air temperature with the facial skin temperature of the subjects, this investigation captured temperature maps of their faces. We used a Lepton 3.5 LWIR camera manufactured by FLIR, with a nominal resolution of 0.05 K and a nominal error of less than 5%. A Purethermal 2 I/O module produced by GroupGets was used to transfer the data to a computer. To accurately measure the temperature, the camera was calibrated following the instructions provided by the manufacturer [44], and three images were captured at once to acquire consistent data. Furthermore, the camera was pointed directly towards the subject and the distance between subject and camera was maintained at 30 cm for consistency.

For face detection, this investigation used the Haar-cascade model developed by Viola and Jones [43]. This method required less computational power and time than the CNN. To implement the face detection, we used Python as the programming language and OpenCV as the library. Because the Haar-cascade detection model was already available and is universal, there was no need to train it. At this point of study, the face detection was not able to detect partial face of a subject, therefore, the subject was required to look at the LWIR camera for a full-face capture during the experiment to avoid measurement error.

This investigation used the office and preparation room described in the previous section to collect air temperature, mean facial skin temperature, and thermal sensation data. The data collection procedure had the same preparation phase as discussed in Section 2.2 and the procedure after preparation was as follows. After a subject entered the office with air temperature at 23°C, the

subject spent 10 minutes acclimating to the environment. The subject then reported the first TSV, and a thermal image of the face was captured for measurement of the mean facial skin temperature. We then changed the thermostat setpoint by +1 or -1 K. After changing the thermostat, we measured the mean facial skin temperature and recorded the corresponding TSV every five minutes, because the room temperature would exhibit an observable obvious change within this period. For each measurement, three thermal images were captured to ensure accuracy. During the experiment, this study controlled the air temperature within the range of 20°C to 26°C, to produce TSV values that varied from -2 to 2 for each subject. With the collected data, we could then obtain each occupant's mean facial skin temperature at the individual TSV values. By collecting data from different subjects, we could determine the overall range in mean facial skin temperature for each TSV and use it to control the temperature setpoint of the HVAC system.

2.4 HVAC control strategy and validation

As the existing HVAC control strategy did not incorporate the mean facial skin temperature or the clothing level, this study designed a new strategy. The fundamental logic was to raise the temperature setpoint by 1 K when the measured mean facial skin temperature was below the lower bound of the comfortable range and decrease the temperature setpoint by 1 K when the measured mean facial skin temperature was above the higher bound of the comfortable range. If the mean facial skin temperature was in the comfortable range, the setpoint temperature was set to the air temperature at that time to maintain comfort. However, because a change in air temperature may occur slowly, it would be possible to overheat or overcool the room by following this logic alone. To avoid such a scenario, an enhanced logic was applied. The enhanced control strategy compared the temperature setpoint with the air temperature before each setpoint-change decision. The setpoint was changed only if the air temperature had reached the setpoint temperature and the mean facial skin temperature was not in the comfortable range. Fig. 4 provides the flowchart for the enhanced logic.

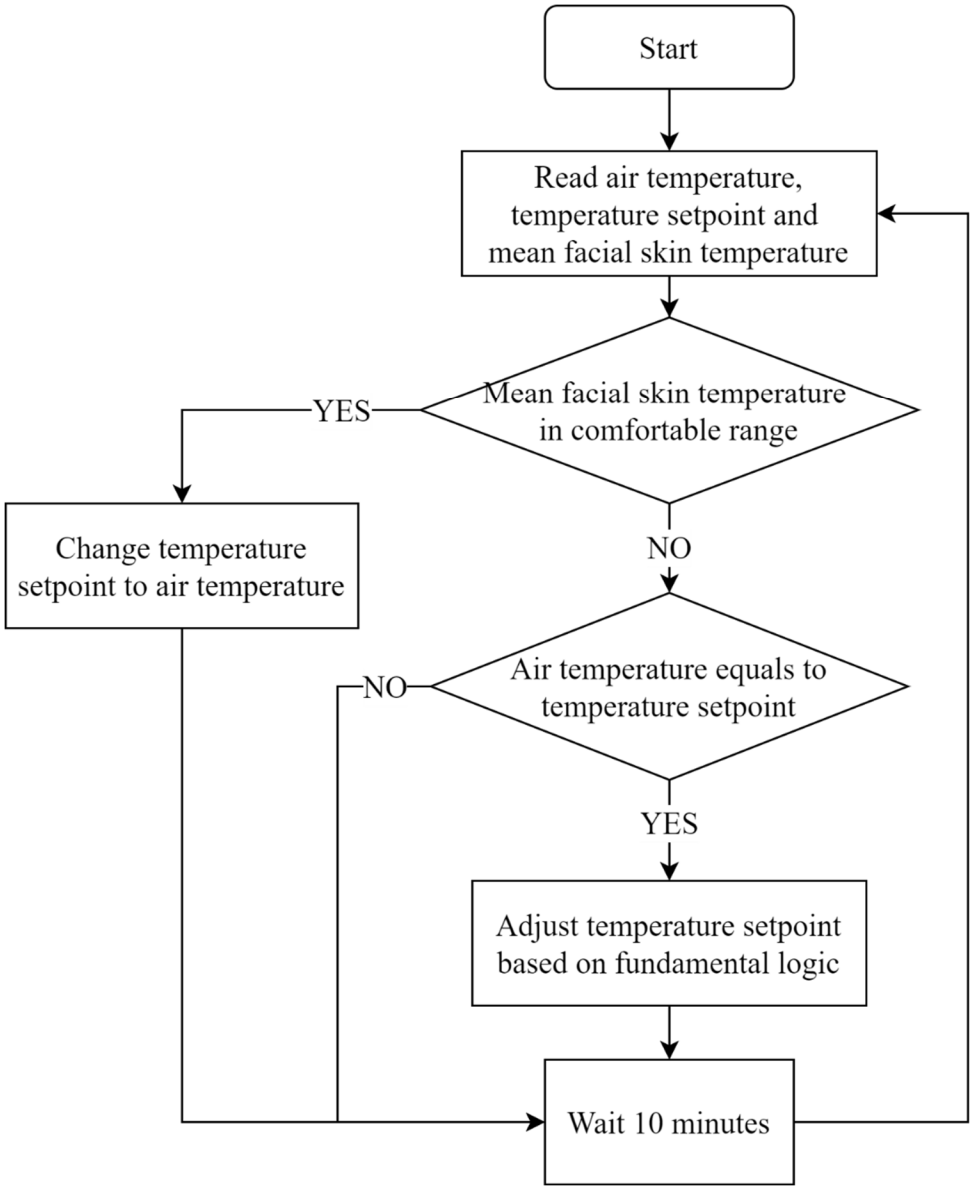

Figure 4. Control strategy for HVAC system using mean facial skin temperature.

This study tested the control strategy in the room shown in Fig. 2. The tests measured the air temperature with the same data logger, the mean facial skin temperature with the Lepton LWIR 3.5 camera, and clothing level with the Logitech RGB camera. We used the same questionnaire to collect the subjects' TSV.

The procedure for the tests was as follows. First, the clothing level of a subject was used to set the initial temperature setpoint in the BAS. The subject waited in another room until the temperature in the test room reached the setpoint. The subject then entered the test room and began a 10-minute acclimation period. The mean facial skin temperature was recorded as an input to the control system. The setpoint temperature of the HVAC system was adjusted accordingly, following the improved logic. Meanwhile, the subject continued to record the TSV. The test procedure was repeated every 10 minutes for the duration of the one-hour experiment. During the tests, to maintain a constant metabolic rate, the subjects performed activities such as typing and reading.

3. Results

This section first provides the results of the clothing-level measurements and the determination of comfortable air temperature for different clothing levels. Next, the relationship between mean facial skin temperature and thermal comfort is revealed. Finally, we present the results of our validation of the control strategy for the HVAC system. Note that results in section 3.2 and section 3.3 were obtained from two subject groups and two independent experiments, the procedures for these two sections can be referred to section 2.2 and section 2.3, respectively. The total participants to this study were 88 college aged students.

3.1 Clothing-level classification

With the hyperparameters from Table 1, training the clothing-level image classification model required 4,334 seconds on a laptop. Fig. 5 depicts the average training loss and average training accuracy for each epoch during the training, represented by solid and dashed lines, respectively. As shown in the figure, the initial training loss was 1.69, and it continued to decrease until it reached 0.68 at the 60th epoch. Meanwhile, the initial training accuracy was 0.35, it increased up to 0.92 at the 60th epoch. The training accuracy indicates the proportion of data in the training dataset that was correctly classified by the model. Thus, the high accuracy at the end of the training proved that the image classification model had been successfully trained for clothing-level classification.

Figure 5. Training results of clothing-level image classification model.

After the model had been trained, it was tested in the labeling of 50 new images captured in offices. This process was designed to validate the use of the image classifier for images it had never seen before. Three examples of the new images are displayed in Fig. 6. The true clothing levels for the three images were 0.3, 0.8 and 0.5 clo, respectively. Table 3 lists the classification results for these images. The level of confidence represents the likelihood that the image displayed the

corresponding clothing level. For each sample image, the highest likelihood (highlighted in the table) indicates the clothing level that was correctly identified by the classifier.

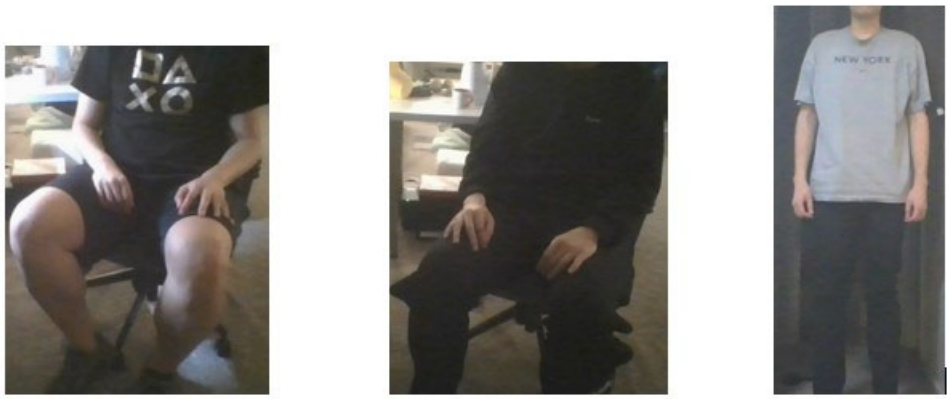

(a) (b) (c)

Figure 6. Sample images for testing the trained classification model.

Table 3. Classification results for the sample images.

		Level of Confidence		
		Fig. 6(a)	Fig. 6(b)	Fig. 6(c)
Clothing Level	0.3 clo	0.826	0.002	0.051
	0.4 clo	0.005	0.031	0.312
	0.5 clo	0.005	0.017	0.591
	0.6 clo	0.098	0.014	0.002
	0.7 clo	0.012	0.147	0.004
	0.8 clo	0.054	0.789	0.040

Table 4 shows the overall classification performance for the 50 images that the classifier had not previously encountered. The classifier correctly classified 86% of the images, most of which were classified with a high level of confidence. These results demonstrate that the CNN was able to non-invasively measure the clothing level. We realized that the upper limit of the clothing level was only 0.8 clo that could be too low for covering all people. Since this investigation was not a comprehensive thermal comfort study but demonstration of a different approach to evaluate thermal comfort, the clothing data can be expanded in the future.

Table 4. Performance of the trained image classification model.

Result	**Number of images**
Correct (level of confidence > 70%)	35
Correct (70% > level of confidence > 50%)	8

Wrong	7

294

295 **3.2 Comfortable air temperature at different clothing levels**

296 This study collected more than 450 data points from 41 college students on comfortable air
297 temperature from subjects with clothing levels ranging from 0.3 to 0.8 *clo*. According to the raw
298 data in Fig. 7, the comfortable air temperature was different for different clothing levels, and it
299 increased as clothing level decreased.

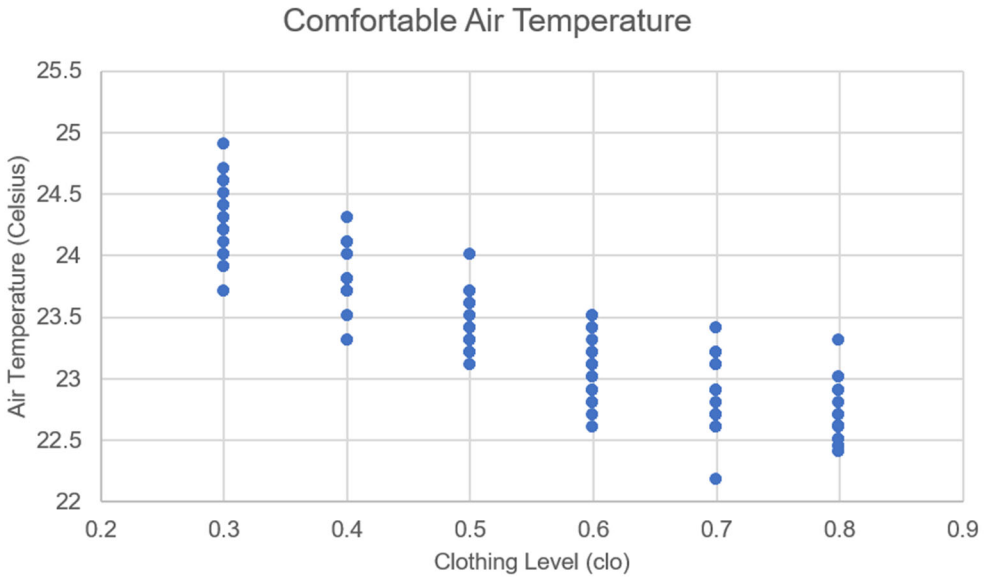

300

301 Figure 7. Raw data on comfortable air temperature.

302

303 From the collected data, it was possible to determine a single comfortable air temperature for each
304 clothing level. Therefore, the average air temperature at each clothing level was computed along
305 with its standard deviation for examination of the data distribution, as shown in Table 5. The mean
306 air temperature in the table indicates that the comfortable air temperature increased as the clothing
307 level decreased. When clothing level decreased, the area of skin exposed to the environment
308 increased, which in turn increased the total amount of heat exchanged between the human body
309 and the environment. To feel comfortable, the subject required a warmer environment because it
310 reduced the temperature difference between the subject and the environment, thus preserving the
311 heat balance. The standard deviation indicates that the results were consistent.

312 Table 5. Comfortable air temperature for different clothing levels.

Clothing Level (clo)	0.3	0.4	0.5	0.6	0.7	0.8
Average Air Temperature (°C)	24.3	23.8	23.4	23.1	22.8	22.6
Standard Deviation (°C)	0.29	0.34	0.23	0.29	0.33	0.24

313

To elucidate the findings, this study also calculated PMV and PPD using the experimental data, as shown in Table 6. The calculated PMV values were all negative, indicating that the actual air temperature was lower than that predicted by the model. The average PMV for the six clothing levels was -0.58, pointing to a slightly uncomfortable environment. The PPD indicates the percentage of people that may feel dissatisfied under the given environment. The average PPD for the six clothing levels was 12.83%. The PPD reached a maximum when the clothing level was 0.3 *clo*. One reason for the high dissatisfaction may have been the assumption that the mean radiant temperature was the same as the air temperature. Because in summer, the outdoor air temperature was higher, and the office used for data collection had one exterior wall, the mean radiant temperature would have been higher than the air temperature in summer. Therefore, the real operative temperature would have been higher, which would have brought PMV closer to zero and reduced the PPD. We can apply similar reasoning to the PMV and PPD for 0.4 *clo* and 0.5 *clo*, which were also common clothing levels in summer. Hence, the comfortable air temperature under different clothing levels agrees reasonably well with the PMV and PPD values in the office environment.

Table 6. PMV and PPD determined at the measured air temperature and clothing level.

Clothing Level (clo)	**0.3**	**0.4**	**0.5**	**0.6**	**0.7**	**0.8**
Average Air Temperature (°C)	24.3	23.8	23.4	23.1	22.8	22.6
Calculated PMV	-0.86	-0.77	-0.66	-0.52	-0.4	-0.27
Calculated PPD	21%	17%	14%	11%	8%	6%

3.3 Relationship between mean facial skin temperature and thermal comfort

Temperature maps of subjects' faces were captured according to the method described in Section 2.3. Fig. 8 provides an example of the maps that were obtained. The enclosed area in the figure was detected as a human face. This study used a threshold of 26°C to eliminate the effect of background, hair, and glass. By using the threshold, the temperature calculation program would only calculate the temperature higher than the threshold to reduce the measurement noise. For example, in Fig. 8, the temperature of the glass would be lower than 26 °C, thus, the temperature of it did not affect the final calculation results. The background in the green rectangle and small hair parts on the right top corner were also ignored during temperature calculation. Then, the program calculated the mean value in the enclosed area to determine the mean facial skin temperature. Determining the facial skin temperature from the map required five seconds. This result demonstrates the effectiveness and practicality of combining the LWIR camera and face detection program to calculate the mean facial skin temperature.

Figure 8. Detection of a face area for determining facial skin temperature.

After validating the LWIR camera and the face detection program, this study collected data on mean facial skin temperature for correlation with thermal comfort. Fig. 9 depicts the correlation, where the horizontal axis represents the thermal sensation vote, and the vertical axis represents the mean facial skin temperature measured by the camera.

The results displayed in Fig. 9(a) consist of 225 TSV data points from -2 to 2 of 30 college students. We described the data using a linear regression line which had a R^2 value as 0.86. By using a boxplot shown as Fig. 9(b), we can see the mean value (represented by the cross mark) is close to the median for each TSV indicating a normal distribution. Under the air temperature range from 20 to 26 °C, subjects felt neutral most of the time; therefore, TSV = 0 had the most data points. The other TSV values all had similar numbers of data points. The data exhibits a clear trend: as TSV increased, which means that the occupant felt warmer, the mean facial skin temperature increased. When the TSV decreased, which means that the occupant felt cooler, the mean facial skin temperature decreased. The minimum recorded temperature was 30.5 °C for TSV = -2, and the maximum recorded temperature was 33.78 °C for TSV = 2.

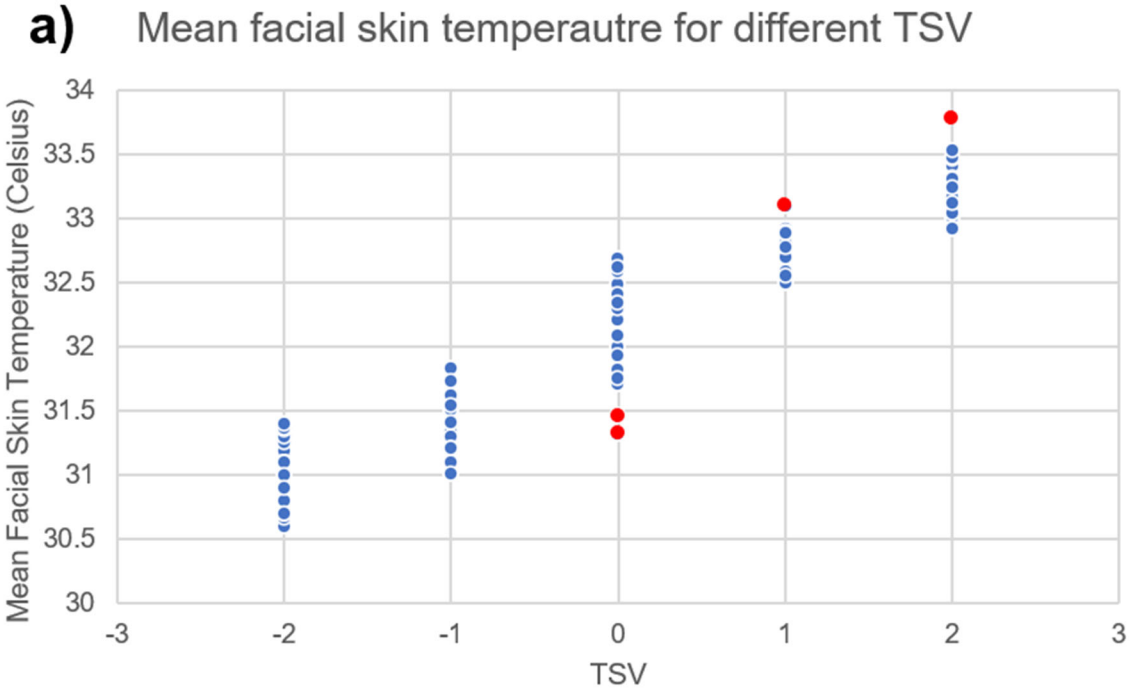

361

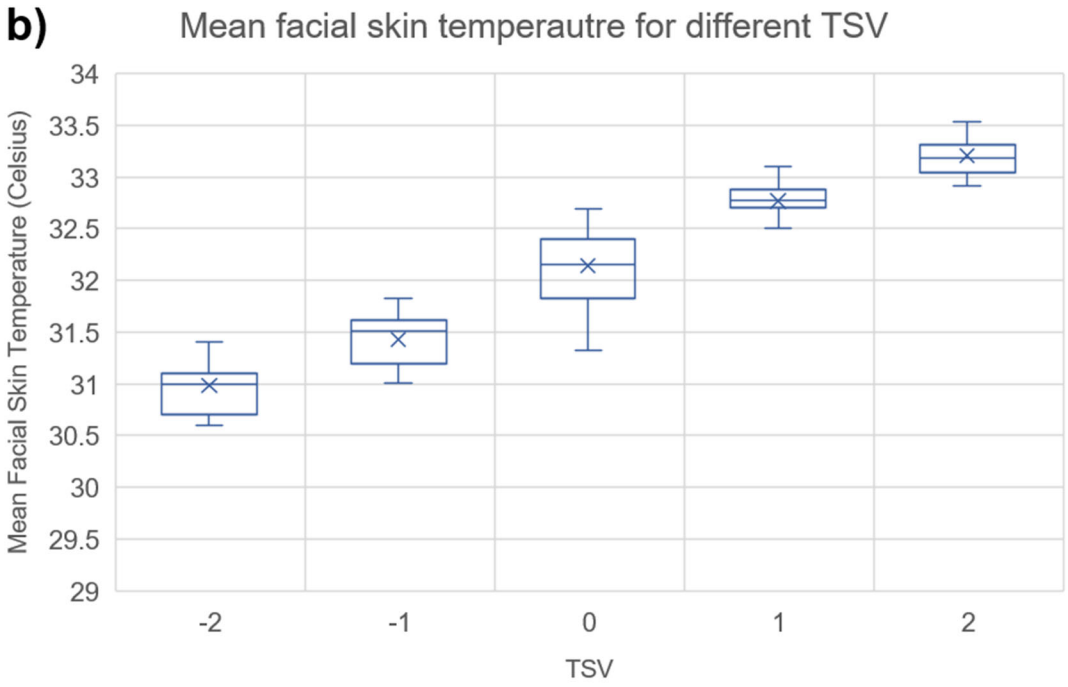

362

363 Figure 9. Mean facial skin temperature: a) raw data collected for TSV values from -2 to 2. b) box
364 plot representation of data collected for TSV values from -2 to 2.

365 Meanwhile, in-group variation existed for all TSV values because the skin temperature was
366 regulated by the body's thermoregulation system and dependent on individual physiological
367 parameters such as age and gender, which can differ among individuals. There were only a few

outliers (represented by red dots in Fig. 9) in the collected data, which indicates that, for most people, the mean facial skin temperature occurred in the same range for different TSV values.

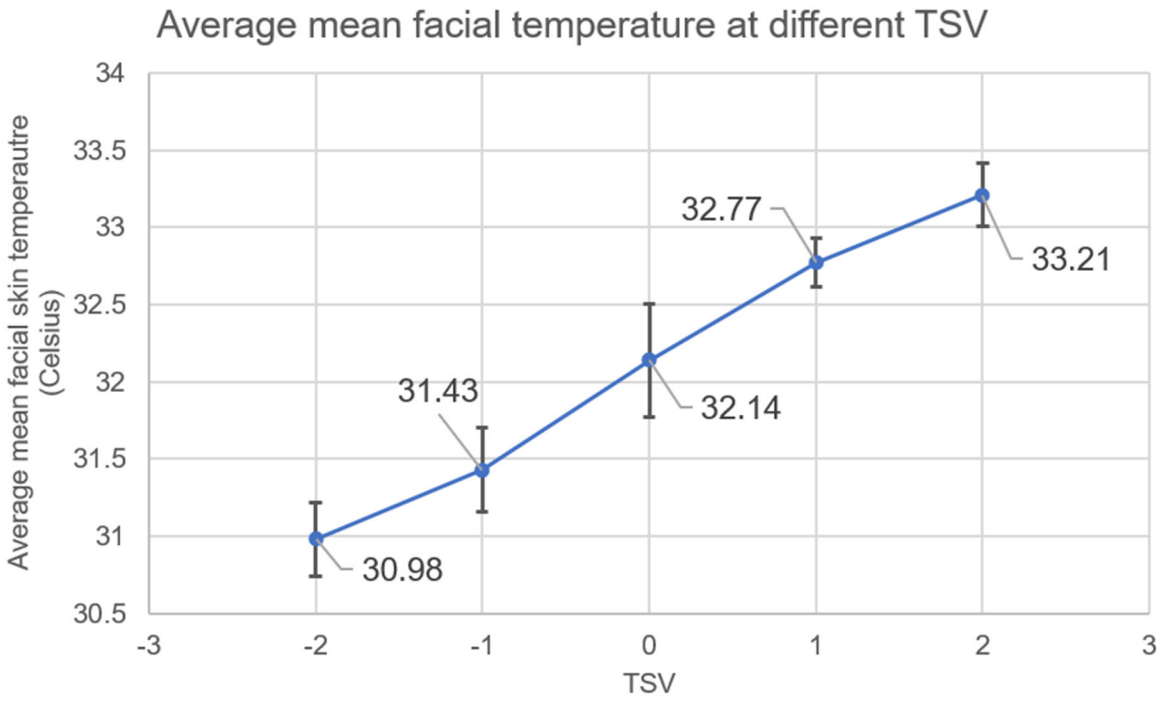

Figure 10. Average mean facial skin temperature at different TSV values.

Next, Fig. 10 shows the average mean facial skin temperature at different TSV values. The vertical line at each data point indicates the 95% confidence interval for that value. The calculation of this interval assumed a normal distribution within each group. The span of the interval was the widest for TSV = 0, indicating a large variation in the individual mean facial skin temperature. Meanwhile, the internal span was the smallest for TSV = 1. This indicates a small variation in the individual measurement. Specifically, at TSV = 0, the mean facial skin temperature ranged from 31.7 to 32.5 °C, at TSV = -1 the range was 31.7 to 31.16 °C, at TSV = -2, the range was 30.74 to 31.22 °C, at TSV = 1 the range was 32.62 to 32.92°C and at TSV = 2, the range was 33.01 to 33.41 °C. The results clearly demonstrate a strong correlation between TSV and facial skin temperature.

From this dataset, we extracted the mean facial skin temperature range at each TSV and used it to deduce how occupant would like the room temperature to change. For example, when the measured mean facial skin temperature was 32.1 °C, we assumed the occupant was feeling comfortable and would not want the air temperature to change. Thus, we maintained air temperature setpoint constant. On the other hand, if the mean facial skin temperature was 31.2 °C, which would rely in TSV = -1 or -2. In this case, we could not determine the accurate setpoint for the subject, but we could increase the setpoint by 1 K and wait to see how the subject felt after adjusting the setpoint. If after changing the setpoint, the subject's mean facial skin temperature was still lower than comfortable range, we would increase the setpoint by 1 K again and repeat this procedure to make subject feel comfortable. Since this control method was continuous and it could monitor the real-time mean facial skin temperature, the adjustment would be quite timely. As for the period of

uncomfortable time, it would vary based on the HVAC system; if a system took 20 minutes to raise 1 K of air temperature, then the uncomfortable period would be more than 20 minutes or longer if multiple adjustment was necessary.

3.4 HVAC control strategy and validation

After facial skin temperature had been correlated with TSV, the HVAC system control strategy shown in Fig. 4 was implemented. This study performed 22 tests with 17 participants to validate the control strategy, as displayed in Table 7. The tests led to three different outcomes. The first outcome was that the subjects were comfortable throughout the whole experiment. The second was that the subjects did not feel comfortable with the initial temperature setpoint, then became comfortable after adjusting the setpoint. In the third group of tests, a comfortable temperature was not identified under this control strategy. Since the first two groups of tests accounted for 91% of the total, we concluded that facial skin temperature could be used to control an HVAC system.

Table 7. Numbers of tests for different outcomes.

Thermal sensation votes	**Number of tests**
Neutral (TSV = 0) throughout the whole experiment	14
Initially uncomfortable (TSV ≠ 0) with the setpoint, then became comfortable (TSV = 0) after changing the setpoint according to facial skin temperature	6
Uncomfortable (TSV ≠ 0) with the control strategy	2

4. Discussion

This study investigated a method for measuring clothing level based on visual content with the use of a convolutional neural network. This study provided a timelier way to determine clothing level comparing to methods mentioned in [35] and [36], because we used real-time images to make prediction. However, the prediction accuracy of the trained CNN model was not extremely high. This was because the CNN used in this study was not fine-tuned to the specific task. Fine-tuning the pre-trained CNN model would have consumed more computational power and time and would have required a more detailed dataset than the one we had. Therefore, we did not fine-tune the model before training.

Furthermore, the trained model had the potential for overfitting because the dataset was small, which limited the training effectiveness in each epoch. It would be ideal to train the network by using more steps per epoch, rather than more epochs. Another weakness was the use of the method to calculate clothing level, as ASHRAE has done, because clothing level reflects only the total clothing and not the clothing distribution. For example, when a person wears a short-sleeved shirt, the person's arm has a greater chance of a cold/hot feeling than does the torso. Our method of clothing-level prediction does not reflect an uneven distribution of clothing. The ability to determine the distribution would lead to a more personalized environment. What is more, the RGB camera would compromise the privacy which needed to be handled in actual application. Using a special server to storage the image or destroy image after usage is a potential solution.

As for thermal comfort study, the results had similar trend with those in [14-15, 24-26]. However, the absolute value for each specific TSV was different due to different measurement method and test group. Our thermal comfort experiment was limited to college students. Such a bias in test-

subject selection would affect the results because age contributes to physiological and psychological differences among people. For example, the metabolic rate of a young person would be higher than that of an elderly person, making the younger people feel less cold. Similarly, a younger person might have a higher tolerance for a cooler environment, while an older person might prefer a warmer environment.

Another issue was the location of the LWIR camera. The subjects in our investigation had to look at the camera every 10 minutes to take measurements. Such interruptions would not be ideal in a real environment. Also, if a subject was not facing the camera squarely, the face detection method would not be able to find the face, and no facial temperature would be measured. Therefore, it might be helpful to have multiple cameras capturing images of the subjects. Moreover, using multiple cameras to capture the image and average the results could also reduce the error induced by each camera.

Overshooting the air temperature was another potential problem, especially when the test room was being heated. The heat was provided by a radiator, which continued to emit heat even after it had been turned off by the control system. Thus, the room air temperature could not be maintained as our desire. Such situation would make occupants uncomfortable.

Moreover, energy consumption and cost of operation with the control strategy developed in this study were not studied. This strategy introduced new equipment and algorithm such as CNN, which may require a new HVAC control infrastructure for security and data processing. Therefore, the cost may increase or decrease comparing to traditional systems and worth further investigation.

5. Conclusions

This investigation developed a new method to control the thermal environment in an office in order to make it comfortable for occupants. The following conclusions were reached:

(1) This study employed an RGB camera combined with a convolutional neural network to determine occupants' clothing levels in real time. After the classifier had been trained with 300 images per clothing level, it was able to correctly classify 84% of the images by clothing level with a high level of confidence.

(2) This investigation found a correlation between comfortable air temperature and clothing level. Comfortable air temperature resulted in PMV of -0.58 for the six clothing levels studied. This investigation assumed the surrounding temperature to be the same as the air temperature, which would have contributed some error to the results.

(3) This study used an LWIR camera to measure mean facial skin temperature. When a subject felt thermally neutral, the mean facial skin temperature was between 31.7 and 32.5 °C.

(4) This investigation used the facial skin temperature to control an HVAC system. According to tests of 17 subjects in 22 sessions, 90.9% of the subjects felt comfortable under the control strategy.

Acknowledgements

The testing of human subjects in this study was approved by the Purdue University Institutional Review Board with an exemption according to protocol #1811021298.

References

[1] Klepeis, N. E., Nelson, W. C., Ott, W. R., Robinson, J. P., Tsang, A. M., Switzer, P., … Engelmann, W. H. (2001). The National Human Activity Pattern Survey (NHAPS): A resource for assessing exposure to environmental pollutants. *Journal of Exposure Science & Environmental Epidemiology*, *11*(3), 231–252.

[2] Földváry Ličina, V., Cheung, T., Zhang, H., de Dear, R., Parkinson, T., Arens, E., Chun, C., Schiavon, S., Luo, M., Brager, G., Li, P., & Kaam, S. (2018), ASHRAE Global Thermal Comfort Database II, v4, *UC Berkeley,* Dataset

[3] ANSI/ASHRAE. (2017). Standard 55: 2017, Thermal Environmental Conditions for Human Occupancy. *ASHRAE*.

[4] Enescu, D. (2017). A review of thermal comfort models and indicators for indoor environments. *Renewable and Sustainable Energy Reviews*, *79*, 1353–1379.

[5] Fanger, P. O. (1982). *Thermal Comfort: Analysis and Applications in Environmental Engineering*. Malabar, FL: Krieger.

[6] McIntyre, D. A. (1978). Three approaches to thermal comfort. *ASHRAE Transactions*, *84*, 101–109.

[7] Schiavon, S., & Melikov, A. K. (2008). Energy saving and improved comfort by increased air movement. *Energy and Buildings*, *40*(10), 1954–1960.

[8] Dear, R. J., Akimoto, T., Arens, E. A., Brager, G., Candido, C., Cheong, K. W., . . . Zhu, Y. (2013). Progress in thermal comfort research over the last twenty years. *Indoor Air*, *23(6)*, 442-461.

[9] Kim, J., Schiavon, S. & Brager, G. (2018). Personal Comfort Models – A New Paradigm in Thermal Comfort for Occupant-Centric Environmental Control. *Building and Environment, 132,* 114–24

[10] Indraganti, M., Ooka, R., Rijal, H. B., & Brager, G. S. (2014). Adaptive model of thermal comfort for offices in hot and humid climates of India. *Building and Environment*, *74*, 39–53.

[11] Fanger, P. O., & Toftum, J. (2002). Extension of the PMV model to non-air-conditioned buildings in warm climates. *Energy and Buildings*, *34*(6), 533–536.

[12] Xu, W., Chen, X. & Zhao, J. (2010). An adaptive Predicted Mean Vote (aPMV) model in office. *2010 International Conference on Mechanic Automation and Control Engineering*.

[13] Ogbonna A. C., & Harris D. J. (2008). Thermal comfort in sub-Saharan Africa: Field study report in Jos–Nigeria. *Applied Energy*, *85*, 1–11.

[14] Choi, J.-H., & Loftness, V. (2012). Investigation of human body skin temperatures as a bio-signal to indicate overall thermal sensations. *Building and Environment*, *58*, 258–269.

[15] Choi, J.-H., & Yeom, D. (2017). Study of data-driven thermal sensation prediction model as a function of local body skin temperatures in a built environment. *Building and Environment*, *121*, 130–147.

[16] Salehi, B., Ghanbaran, A. H., & Maerefat, M. (2020). Intelligent models to predict the indoor thermal sensation and thermal demand in steady state based on occupants' skin temperature. *Building and Environment, 169,* 106579

[17] Jazizadeh, F., & Jung, W. (2018). Personalized thermal comfort inference using RGB video images for distributed HVAC control. *Applied Energy*, *220*, 829–841.

[18] Yi, B., & Choi, J.-H. (2015). Facial skin temperature as a proactive variable in a building thermal comfort control system. *Sustainable Human–Building Ecosystems*, 117–125.

[19] Xiong, J., Lian, Z., Zhou, X., You, J., & Lin, Y. (2016). Potential indicators for the effect of temperature steps on human health and thermal comfort. *Energy and Buildings*, *113*, 87–98.

[20] Choi, J.-H., Loftness, V. & Lee, D.-W. (2012). Investigation of the possibility of the use of heart rate as a human factor for thermal sensation models. *Building and Environment 50,* 165-175

[21] Kizito N. Nkurikiyeyezu, Yuta Suzuki, Guillaume F. Lopez. (2018). Heart rate variability as a predictive biomarker of thermal comfort. *Journal of Ambient Intelligence and Humanized Computing, 9.5,*1465-1477.

[22] Liu, S., Schiavon, S., Das, H. P., Jin, M., & Spanos, C. J. (2019). Personal thermal comfort models with wearable sensors. *Building and Environment*, *162*, 106281.

[23] Li, D., Menassa, C. C., & Kamat, V. R. (2018). Non-intrusive interpretation of human thermal comfort through analysis of facial infrared thermography. *Energy and Buildings*, *176*, 246–261.

[24] Cosma, A. C., & Simha, R. (2018). Thermal comfort modeling in transient conditions using real-time local body temperature extraction with a thermographic camera. *Building and Environment*, *143*, 36–47.

[25] Cosma, A. C., & Simha, R. (2019). Machine learning method for real-time non-invasive prediction of individual thermal preference in transient conditions. *Building and Environment*, *148*, 372–383.

[26] Wang, F., Zhu, B., Li, R., Han, D., Sun, Z., Moon, S., … Yu, W. (2017). Smart control of indoor thermal environment based on online learned thermal comfort model using infrared thermal imaging. *2017 13th IEEE Conference on Automation Science and Engineering (CASE)*.

[27] Kontes, G., Giannakis, G., Horn, P., Steiger, S., & Rovas, D. (2017). Using thermostats for indoor climate control in office buildings: The effect on thermal comfort. *Energies*, *10*(9), 1368.

[28] Arens, E., Humphreys, M. A., Dear, R. J., & Zhang, H. (2010). Are 'class A' temperature requirements realistic or desirable? *Building and Environment*, *45*(1), 4–10.

[29] Nicol, J., & Humphreys, M. (2002). Adaptive thermal comfort and sustainable thermal standards for buildings. *Energy and Buildings*, *34*(6), 563–572.

[30] Brager, G., Zhang, H., & Arens, E. (2015). Evolving opportunities for providing thermal comfort. *Building Research & Information*, *43*(3), 274–287.

[31] Peffer, T., Pritoni, M., Meier, A., Aragon, C., & Perry, D. (2011). How people use thermostats in homes: A review. *Building and Environment*, *46*(12), 2529–2541.

[32] Derrible, S., & Reeder, M. (2015). The cost of over-cooling commercial buildings in the United States. *Energy and Buildings*, *108*, 304–306.

[33] Yao, R., Li, B., & Liu, J. (2009). A theoretical adaptive model of thermal comfort – Adaptive Predicted Mean Vote (aPMV). *Building and Environment*, *44*(10), 2089–2096.

[34] Gagge, A. P., Stolwijk, J. A. J., & Nishi, Y. (1971). An effective temperature scale based on a simple model of human physiological regulatory response. *ASHRAE Transactions*, *77*(1), 247–262.

[35] Schiavon, S., & Lee, K. H. (2013). Dynamic predictive clothing insulation models based on outdoor air and indoor operative temperatures. *Building and Environment*, *59*, 250–260.

[36] Liu, W., Yang, D., Shen, X., & Yang, P. (2018). Indoor clothing insulation and thermal history: A clothing model based on logistic function and running mean outdoor temperature. *Building and Environment*, *135*, 142–152.

[37] Carvalho, P. M. D., Silva, M. G. D., & Ramos, J. E. (2013). Influence of weather and indoor climate on clothing of occupants in naturally ventilated school buildings. *Building and Environment*, *59*, 38–46.

[38] Schindler, A., Lidy, T., Karner, S., & Hecker M. (2018). Fashion and apparel classification using convolutional neural networks. *arXiv preprint arXiv:1811.04374*

[39] Sandler, M., Howard, A., Zhu, M., Zhmoginov, A., & Chen, L.-C. (2018). MobileNetV2: Inverted residuals and linear bottlenecks. *2018 IEEE/CVF Conference on Computer Vision and Pattern Recognition*.

[40] TensorFlow (n.d.). Transfer learning with a pretrained ConvNet, *TensorFlow,* https://www.tensorflow.org/tutorials/images/transfer_learning.

[41] Smith, L.N. (2018). A disciplined approach to neural network hyper-parameters: Part 1 -- Learning rate, batch size, momentum, and weight decay. *arXiv*, 1803.09820

[42] Liu, H., Liao, J., Yang, D., Du, X., Hu, P., Yang, Y., & Li, B. (2014). The response of human thermal perception and skin temperature to step-change transient thermal environments. *Building and Environment*, *73*, 232–238.

[43] Viola, P., & Jones, M. (n.d.). Rapid object detection using a boosted cascade of simple features. *Proceedings of the 2001 IEEE Computer Society Conference on Computer Vision and Pattern Recognition. CVPR 2001*.

[44] FlIR Systems (n.d.). *Technical Documentation: FLIR Lepton with Radiometry QuickStart Guide* https://www.flir.com/products/lepton/

[45] Russell, S. J., & Norvig, P. (2015). *Artificial intelligence: A modern approach*.